

1 Supplementary figure

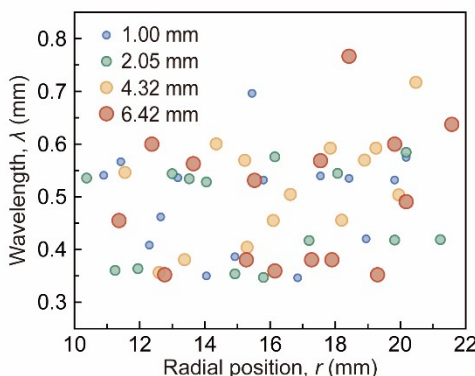


Fig. S1 Wavelength variation trend of pedal waves along radial coordinate r while collecting varying-sized particles.

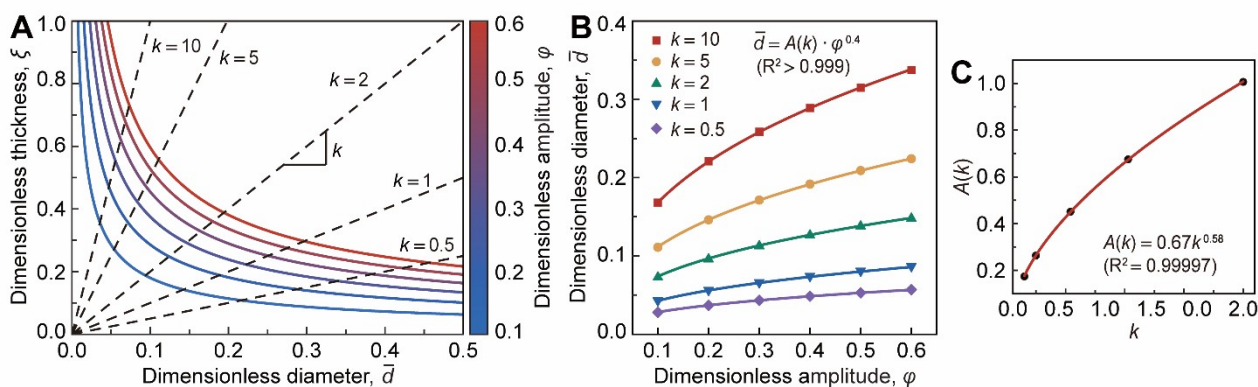


Fig. S2 (A) Pencil of ξ - \bar{d} curves and orthogonal trajectories. (B)-(C) Relationship between \bar{d} and φ in varying slopes k of orthogonal trajectories.

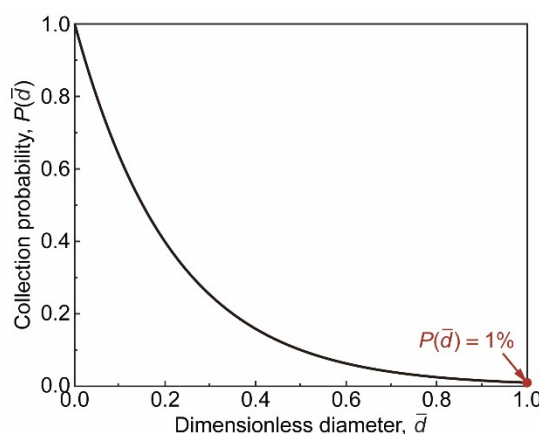


Fig. S3 Probability of particle collection satisfies the exponential distribution. The probability $P(\bar{d})$ is set to 1% at $\bar{d} = 1.0$, which means an imaginarily large particle located in a diameter equivalent to the funnel radius cannot to collect by the snail.

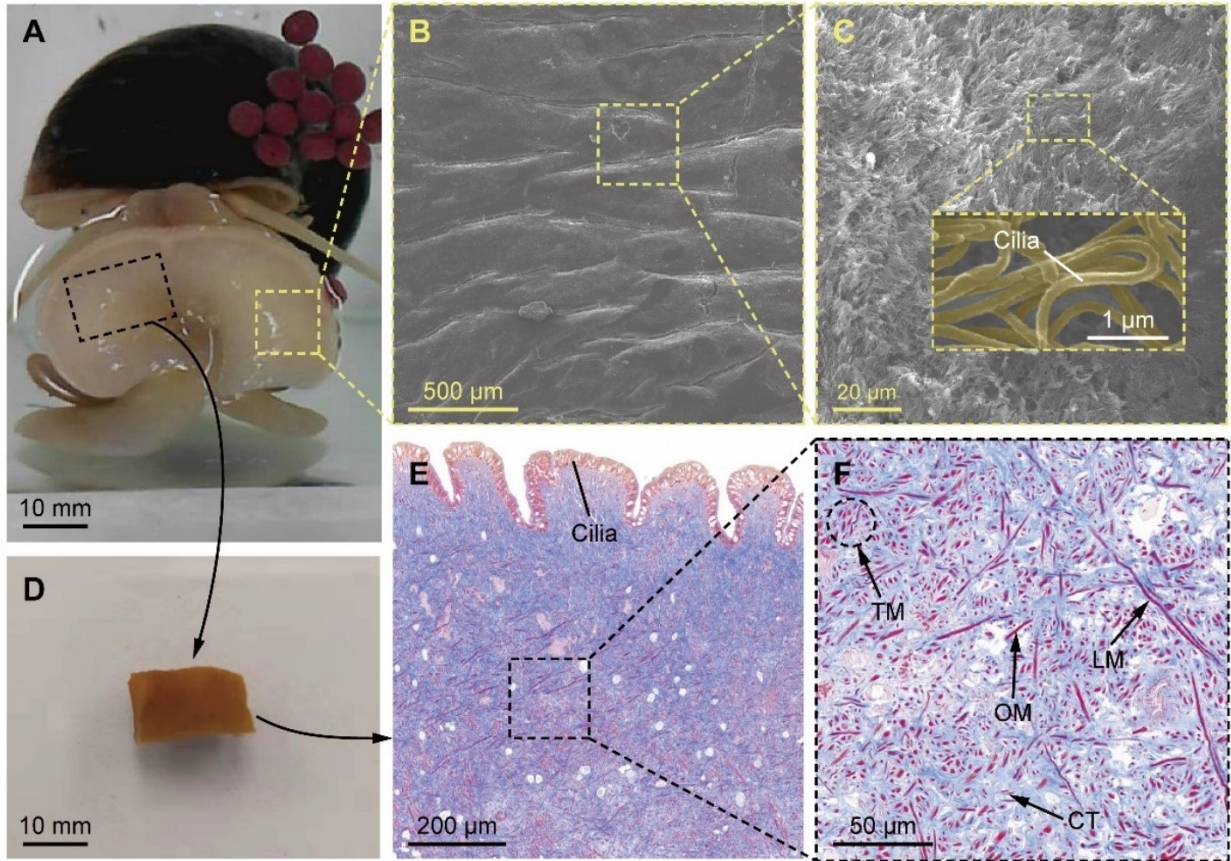


Fig. S4 (A) Natural feeding behavior of a water snail that uses its foot to collect particles floating on the water surface. (B)-(C) SEM images of the snail foot surface. The cilia are densely distributed on textured surface of snail foot. (D) Samples for preparing foot muscle slices. (E)-(F) Distribution of foot muscles of the snail. Thin longitudinal section of the muscle stained with masson dye solution, showing transverse muscles (TM), oblique muscles (OM), longitudinal muscles and connective tissue (CT) surrounding the muscles.

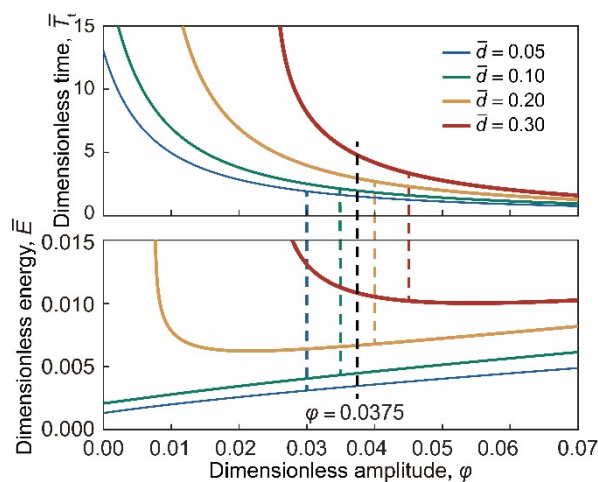


Fig. S5 Transport time and energy consumption when transporting different particles by varying

amplitudes. The dotted line is used to compare the transport time and energy consumption at a specific amplitude, in which the colored lines indicate that varying amplitudes are used to transport different particles and the black line indicate that a specific amplitude is used to transport.

2 Supplemental information

3 S1. Particle velocity

4 Considering a two-dimensional situation, in the frame fixed to the foot surface wave,
 5 applying the lubrication approximation to the incompressible Navier-Stokes equation,
 6 we have

$$\frac{\partial p}{\partial r} = \mu \frac{\partial^2 u_r}{\partial z^2}, \quad \frac{\partial p}{\partial z} = 0, \quad \text{Equation S1}$$

7 in which u_r is the component of velocity along the r -direction, and p is the pressure.
 8 First, we rationalize the flow of mucus covering the foot surface. The boundary
 9 conditions for Equation S1 can be expressed as $u_r = -V_w$ at $z = f$, as well as $\partial u_r / \partial z = 0$
 10 at $z = h$, where f and h are the vertical position of the foot surface and the gas-liquid
 11 interface, respectively. Since p depends upon merely r rather than z , $\partial p / \partial r$ can be written
 12 as dp/dr . Integrating Equation S1 in the r -direction twice with respect to z , while using
 13 the boundary conditions, we arrive at the velocity of the mucus flow as

$$u_r = -V_w - \frac{1}{2\mu} \frac{dp}{dr} [(h-f)^2 - (h-z)^2]. \quad \text{Equation S2}$$

14 Further, integrating the velocity with respect to z , we get the rate of volume flow at
 15 each cross-section as

$$q = \int_f^h u_r dz = -V_w(h-f) + \frac{(h-f)^3}{3\mu} \frac{dp}{dr}, \quad \text{Equation S3}$$

16 which is a time-independent constant because the mucus thickness is time-invariant in
 17 the wave frame.

18 When the free surface remains approximately flat and undisturbed, the mucus is
 19 validated to be actuated by the pedal waves, rather than the hydrostatic pressure or
 20 surface tension¹. In other words, the location of the free surface can be approximated

21 as a critical constant h_0 . We may derive a relationship of $h \neq h_0$, otherwise the pressure
 22 would be uniform and there would be no flow on the no-slip surface. There might have
 23 two ultimate states to the free surface location. For the first state where the capillary
 24 number Ca tends to infinity, the interface shape exactly conforms to the wavy shape of
 25 the foot. In the other state with $Ca \approx 0$, the mucus-air interface becomes flat². To get an
 26 approximately flat free surface, the change in mucus thickness is required to satisfy
 27 $|h - h_0| \ll f_0$. According to the momentum equations in the r -direction, viscous stresses
 28 must be balanced by the pressure gradient. By balancing the terms and rearranging, an
 29 approximately flat free surface is given by (3.9) of¹:

$$\frac{\rho g (h_0 - f_0)^2}{\sigma} \gg \frac{\lambda}{f_0} Ca, \quad Ca \equiv \frac{\mu U}{\sigma} \ll \frac{(h_0 - f_0)^2 f_0}{\lambda^3}. \quad \text{Equation S4}$$

30 We consider mucus has the same density and surface tension as water, while being 100
 31 times in viscosity¹. By introducing the numbers of the mucus thickness $H = 1$ mm, the
 32 amplitude $f_0 = 0.1$ mm, and the wavelength $\lambda = 0.5$ mm, we can extend Equation S4
 33 into $Ca \equiv 10^{-3} \ll 0.4$ that satisfies the flat free surface approximation. So, in the
 34 following derivations, h can be replaced by h_0 .

35 The rate of volume flow at each cross section in the laboratory frame is
 36 $Q = q + v_w(h_0 - f)$, then the volume flow averaged by total duration at each cross section

37 can be calculated by integrating over the period: $Q^{mean} = \int_0^T Q dt / T = q + V_w h_0$.

38 Substituting Q^{mean} into Equation S3, and introducing the dimensionless amplitude
 39 $\varphi = f_0/h_0$ and dimensionless volume flow $\theta = Q^{mean}/(V_w h_0)$, we get

$$\frac{h_0^2}{\mu V_w \lambda} dp = \frac{3\varphi \left(\theta - \frac{f}{f_0} \right)}{\lambda \left(\varphi \frac{f}{f_0} - 1 \right)^3} dr. \quad \text{Equation S5}$$

40 Actually, dimensionless amplitude φ is a small quantity. We rewrite right side of

41 Equation S5 by Taylor expansion, keeping it to the order of φ^3 :

$$\frac{h_0^2}{\mu V_w \lambda} dp = \frac{1}{\lambda} \left[3\varphi \left(\frac{f}{f_0} - \theta \right) + 9\varphi^2 \frac{f}{f_0} \left(\frac{f}{f_0} - \theta \right) + 18\varphi^3 \left(\frac{f}{f_0} \right)^2 \left(\frac{f}{f_0} - \theta \right) \right] dr, \quad \text{Equation S6}$$

42 Integrating both sides of the equation simultaneously, we get

$$\frac{h_0^2}{\mu V_w \lambda} \Delta p_\lambda = -3\theta\varphi + \frac{9}{2}\varphi^2 - 9\theta\varphi^3, \quad \text{Equation S7}$$

43 where Δp_λ is the pressure rise within one wavelength. Considering the case of $\Delta p_\lambda = 0$,

44 Equation S7 can be transformed into

$$\theta = \frac{3\varphi}{2(3\varphi^2 + 1)}. \quad \text{Equation S8}$$

45 Next, we rationalize the flow of mucus around the particle. We consider that an
 46 oblate cylindrical floating particle moves radially along the foot without direct contact
 47 with the foot. Assuming that the particle is moving with velocity V_s , the boundary
 48 conditions for Equation S1 can be expressed as $u_r = -V_w$ at $z = f$, as well as
 49 $u_r = V_s - V_w$ at $z = h_s$, in which h_s is the position of the lower surface of the particle. Since
 50 we consider the shape of the particle as an oblate cylinder, the lower surface of the
 51 particle is flat and h_s keeps constant in the static equilibrium. Consistent with the
 52 derivation of the flow of mucus covering the foot surface, we arrive at the velocity of
 53 the local flow in the area between the lower surface of the particle and the surface of
 54 the foot as

$$u_r = -V_w + \frac{z-f}{h_s-f} V_s + \frac{1}{2\mu} \frac{dp}{dr} (z-h_s)(z-f). \quad \text{Equation S9}$$

55 Further, the rate of volume flow at each cross-section can be expressed as

$$q_s = -V_w(h_s - f) + V_s h_s - \frac{(h_s - f)^3}{12\mu} \frac{dp}{dr}, \quad \text{Equation S10}$$

56 which can be averaged by total duration in the laboratory frame is $Q_s^{mean} = q_s + V_w h_s$.

57 Substituting Q_s^{mean} into Equation S10, then introducing the dimensionless amplitude

58 $\varphi_s = f_0/h_s$ and dimensionless volume flow $\theta_s = Q_s^{mean}/(V_w h_s)$ and dimensionless velocity

59 $\chi = V_s/V_w$ into Equation S10, we get

$$\frac{h_s^2}{\mu V_w \lambda} dp = \frac{12\left(\theta_s - \varphi_s \frac{f}{f_0}\right) + 6\left(\varphi_s \frac{f}{f_0} - 1\right)\chi}{\lambda\left(\varphi_s \frac{f}{f_0} - 1\right)^3} dr, \quad \text{Equation S11}$$

60 We rewrite right side of Equation S11 by Taylor expansion, keeping it to the order of

61 φ_s^3 :

$$\begin{aligned} \frac{h_s^2}{\mu V_w \lambda} dp &= \frac{1}{\lambda} \left[6\chi + 12\varphi_s \left(\frac{f}{f_0} \chi + \frac{f}{f_0} - \theta_s \right) \right. \\ &\quad \left. - 6\varphi_s^2 \left(\frac{f}{f_0} \chi + \frac{f}{f_0} - \theta_s \right) + 3\varphi_s^3 \left(\frac{f}{f_0} \chi + \frac{f}{f_0} - \theta_s \right) \right] dr, \end{aligned} \quad \text{Equation S12}$$

62 Integrating both sides of the equation, we get

$$\frac{h_s^2}{\mu V_w \lambda} \Delta p_\lambda = 6\chi - 12\theta_s \varphi_s + (9\chi + 18)\varphi_s^2 - 36\theta_s \varphi_s^3, \quad \text{Equation S13}$$

63 Considering the case of $\Delta p_\lambda = 0$, Equation S13 can be transformed into

$$\theta_s = \frac{6\varphi_s^2 + (3\varphi_s^2 + 2)\chi}{4\varphi_s(3\varphi_s^2 + 1)}. \quad \text{Equation S14}$$

64 In order to match the particle local flow with the global flow, we apply the results

65 above to the axisymmetric configuration of the biological funnel. Extending from two-

66 dimensional case to three-dimensional one, the width-integrated flux of whole foot flow

67 $\Phi = 2\pi r Q^{mean}$ may be equal to the width-integrated flux of particle local flow

68 $\Phi_s = dQ_s^{mean}$. Due to the flow loss of mucus passing through particles in tangential

69 directions, the matching of the two flows should be written as $\Phi_s = (1 - K) \Phi$ where

70 K is a leakiness coefficient K to measure the volume flow loss of mucus between the

71 pedal wave and the lower surface of the particle in other non-radial directions.

72 Expressing the matching of the flow as $2\pi r (1-K) \theta = d\theta_s$ in dimensionless numbers
 73 and substituting Equation S8 and Equation S14 into it, we rearrange it to get

$$\chi = \frac{12\varphi^2\pi(3\varphi^2 + \xi^2)}{(3\varphi^2 + 1)(3\varphi^2 + 2\xi^2)\xi d} (1-K) r - \frac{6\varphi^2}{3\varphi^2 + 2\xi^2}. \quad \text{Equation S15}$$

74 where $\xi = \varphi/\varphi_s = h_s/h_0$ is a dimensionless number characterizing the relative magnitudes
 75 of h_s and h_0 . We introduce two dimensionless numbers $\bar{r} = r/r_0$ and $\bar{d} = d/r_0$, which
 76 characterize the position of the particle on the surface of the foot and the relative size
 77 of the particle and the funnel, respectively, to make all the variables in Equation S15
 78 dimensionless. In a dimensionless frame, the relationship between the velocity and the
 79 radial position on the foot surface of the particle can be expressed as

$$\chi = \frac{12\varphi^2\pi(3\varphi^2 + \xi^2)}{(3\varphi^2 + 1)(3\varphi^2 + 2\xi^2)\xi \bar{d}} (1-K) \bar{r} - \frac{6\varphi^2}{3\varphi^2 + 2\xi^2}. \quad \text{Equation S16}$$

80 S2. The supporting force for mucus

81 To calculate the supporting force provided by the mucus to the particles, we rewrite
 82 Equation S12 as follows

$$\begin{aligned} & \frac{h_0^2}{\mu V_w \lambda} dp \\ & = \frac{1}{\lambda \eta^2} \left[6\chi + 12 \frac{\varphi}{\xi} \left(\frac{f}{f_0} \chi + \frac{f}{f_0} - \right) \right] dr. \end{aligned} \quad \text{Equation S17}$$

83 Substituting Equation S16 into Equation S17 and integrating both sides simultaneously,
 84 we can get the pressure p . To eliminate the effect of time, we calculate the time-
 85 averaged pressure distribution of the water film under the particle according to

86 $p^{mean} = \int_0^T p dt / T$ and arrive at dimensionless time-averaged pressure as

$$\frac{h_0^2}{\mu V_w \lambda} p^{mean} = \frac{18\pi K \varphi^2 (3\varphi^2 + \xi^2)}{\eta^5 (3\varphi^2 + 1) d \lambda} (r_0^2 - r^2), \quad \text{Equation S18}$$

87 in which we confirmed that the constant term due to the integration by setting the
 88 boundary condition $p^{mean}|_{r=r_0} = 0$ and r_0 is the position of the snail foot edge. For
 89 simplification, in the following text, we rewrite p^{mean} as p . Using \bar{r} and \bar{d} to make all
 90 the variables in Equation S18 dimensionless, the dimensionless pressure acting on the
 91 lower surface of the particle along the radial direction of the foot can be expressed as

$$\frac{h_0^2}{\mu V_w r_0} p = \frac{18\pi K \varphi^2 (3\varphi^2 + \xi^2)}{\xi^5 (3\varphi^2 + 1) \bar{d}} (1 - \bar{r}^2). \quad \text{Equation S19}$$

92 S3. Numerical solution of eqn (5)

93 The numerical results show that all $\xi-\bar{d}$ curves exhibit inverse proportional principles
 94 with varying φ . Examining the slope variation of each curve along the coordinate \bar{d} , we
 95 notice that the orthogonal trajectories of $\xi-\bar{d}$ curve family are the lines through the origin
 96 (Fig. S2A). We intend to record the intersections of the curves with orthogonal
 97 trajectories in varying slopes k and express the relationship between \bar{d} and φ at these
 98 points with an approximate equation.

99 First, we assume that \bar{d} is proportional to the power of φ , which can be expressed as

$$\bar{d} = A\varphi^B. \quad \text{Equation S20}$$

100 Fitting \bar{d} with Equation S20 in varying k and comparing the fitting results (Tab. S1), we
 101 notice that the parameter A is sensitive to k , while B is not. Therefore, we keep the
 102 parameter B constant at $B = 0.4$ and rewrite Equation S20 as

$$\bar{d} = A\varphi^{0.4}. \quad \text{Equation S21}$$

103 According to results of Equation S21 fitting (Fig. S2B), we consider A to be a function
 104 of k . To understand the varying in slopes of the orthogonal trajectories, we fit $A(k)$ in a
 105 form of a power function (Fig. S2C), written as

$$A(k) = mk^n. \quad \text{Equation S22}$$

106 Substitute the fitting result into Equation S21, the relationship between \bar{d} and φ can be
 107 expressed as

$$\bar{d} = 0.67k^{0.58} \cdot \varphi^{0.4}. \quad \text{Equation S23}$$

Tab. S1 Results of Equation S20 fitting

k	0.5	1	2	5	10
A	0.174	0.263	0.451	0.675	1.007
$\Delta A/\Delta k$	/	17.8%	18.5%	11.1%	8.8%
B	0.397	0.396	0.394	0.391	0.388
$\Delta B/\Delta k$	/	0.2%	0.2%	0.1%	0.1%
R^2	0.99999	0.99999	0.99998	0.99996	0.99995

108 S4. Transport time and mass intake rate

109 Since $\chi = -\bar{d}\bar{r}/d\bar{t}$ where duration time t is dimensionless to $\bar{t} = t \cdot V_w/r_0$ and the
 110 negative sign indicates that the particle is moving from the edge of the foot to the center
 111 of the foot, we rewrite Equation S16 as

$$-\frac{d\bar{r}}{d\bar{t}} = C_1\bar{r} + C_2, \quad \text{Equation S24}$$

112 where parameters C_1 and C_2 can be expressed as

$$C_1 = \frac{12\phi^2\pi(3\phi^2 + \xi^2)}{(3\phi^2 + 1)(3\phi^2 + 2\xi^2)\xi\bar{d}} (1 - K), \quad \text{Equation S25}$$

$$C_2 = -\frac{6\phi^2}{3\phi^2 + 2\xi^2}.$$

113 We consider that the moment when the particles are transported inward from the edge
 114 of the pedal wave is $\bar{t} = 0$, namely the initial condition of Equation S24 is $\bar{r}|_{\bar{t}=0} = 1$
 115 Solving the equation with this initial condition, we arrive at the explicit relationship
 116 between \bar{r} and \bar{t} as

$$\bar{r} = -\frac{C_2}{C_1} + e^{-C_1\bar{t}} \left(1 + \frac{C_2}{C_1}\right). \quad \text{Equation S26}$$

117 Assuming that the particle is transported to the position $\bar{r} = \bar{r}_t$ and just leave the flat
 118 portion of the funnel at $\bar{t} = \bar{T}_t$, we can rearrange Equation S26 as

$$\bar{T}_t = -\frac{1}{C_1} \ln \left(\frac{\bar{r}_t + \frac{C_2}{C_1}}{1 + \frac{C_2}{C_1}} \right), \quad \text{Equation S27}$$

119 where \bar{T}_t is the dimensionless form of the particle transport time T_t .

120 S5. Energy cost of changing waveforms

121 To quantify energy cost during the snail altering the waveform, we model the snail
 122 foot composed of a linear elastic material. For steady waves, in the case of small
 123 deformation, the dimensionless power that the snail output to maintain the forced
 124 vibration of the foot muscles can be expressed as

$$\varepsilon \sim \frac{32\pi^2 H^2}{16^2 + D^2}, \quad \text{Equation S28}$$

125 in which H and D are dimensionless parameters identifying the characteristic strength
 126 of forced vibration and the stiffness of the foot muscles, respectively³. According to
 127 previous models that specify the wall displacement in a sinusoidal form⁴⁻⁶, we have the
 128 connections between ϕ and D as

$$\frac{\phi}{\phi_0} \sim D \frac{16 \cos\left(\frac{2\pi}{\lambda} r\right) + D \sin\left(\frac{2\pi}{\lambda} r\right)}{16^2 + D^2}. \quad \text{Equation S29}$$

129 Integrating both sides of the equation simultaneously, we get $\phi \sim D$. Therefore, the
 130 dimensionless power can be expressed as

$$\varepsilon \sim \phi^2. \quad \text{Equation S30}$$

131 Further, we can calculate the energy consumption of the snail during a transport by
 132 $E = \varepsilon \cdot \bar{T}_t$ where E is the dimensionless energy consumption. We compared the changes
 133 in dimensionless transport time and dimensionless energy consumption when
 134 transporting the particles in different sizes by different amplitudes (Fig. S5). As the
 135 amplitude increases, the transport time for a single particle will decrease, but the energy

136 consumption will increase, which requires the snail to balance time cost and energy
137 cost. Taking $\bar{d} = 0.05$ as an example, compared with $\varphi = 0.03$, using the amplitude in
138 $\varphi = 0.0375$ can only help the snail save 15.4% of the energy but the snail has to spend
139 29.3% more time to transport the particle.

140 **References**

- 141 1. S. Joo, S. Jung, S. Lee, R. H. Cowie and D. Takagi, *Journal of the Royal Society*
142 *Interface*, 2020, **17**, 20200139.
 - 143 2. S. Lee, J. W. Bush, A. Hosoi and E. Lauga, *Physics of Fluids*, 2008, **20**, 082106.
 - 144 3. D. Takagi and N. Balmforth, *Journal of fluid mechanics*, 2011, **672**, 219-244.
 - 145 4. Y. Fung and C. Yih, 1968.
 - 146 5. A. H. Shapiro, M. Y. Jaffrin and S. L. Weinberg, *Journal of fluid mechanics*,
147 1969, **37**, 799-825.
 - 148 6. T.-F. Zien and S. Ostrach, *Journal of Biomechanics*, 1970, **3**, 63-75.
- 149